Strong Localized Perturbation Theory: Analysis of Localized Solutions to Some Linear and Nonlinear Diffusive Systems

Michael J. Ward (UBC)

Julian Cole Lecture 2022

Joint with former students/PDFs:, Alan Lindsay (Notre Dame), Jia Gou (Riverside), Wes Ridgway (Oxford), Sarafa Iyaniwura (Los Alamos), Tony Wong (Brown)

and collaborators: Juncheng Wei (UBC), Andy Bernoff (Harvey Mudd), Alexei Cheviakov (USask), M.C. Kropinski (SFU), S. Hormozi (Cornell)

Thanks all other students/PDFS/collaborators/ for work on other joint projects:

Victor Brena-Medina (U. Morales), Wan Chen (Google), Daniel Gomez (UPenn), David Iron (Dalhousie), Theo Kolokolnikov (Dalhousie), Iain Moyles (York U.), Merlin Pelz (UBC), Frederic Paquin-Lefebvre (ENS, Paris), Ignacio Rozada (BCCDC), Michele Titcombe (Champlain College), Simon Tse (Trinity Western), Justin Tzou (Macquarie)

Strong Localized Perturbations for PDE

A strong localized perturbation (SLP) induces an $\mathcal{O}(1)$ change in the solution to a PDE in a spatial region of small $\mathcal{O}(\varepsilon)$ extent. However, it's effect can be much larger, i.e. $\mathcal{O}\left(-1/\log\varepsilon\right)$, across the entire domain.

- Eigenvalues of the Laplacian and Bi-Laplacian in domains with holes
- I: Narrow capture problems for a Brownian particle: (Berg-Purcell problem of biophysics)
- II: Localized "far-from-equilibrium" spot patterns for reaction-diffusion systems in the large diffusivity ratio
- III: Localized signalling compartments or "cells" in 2-D coupled by a PDE bulk diffusion field: collective oscillatory dynamics

SLP theory is based on singular perturbation techniques tailored for problems with localized defects: (Dirac singularities, Green's functions are key). SLP reductions often lead to discrete variational problems or DAE systems).

Survey Ref: MJW, *Spots, Traps, and Patches: Asymptotic Analysis of Localized Solutions to some Linear and Nonlinear Diffusive Processes*, Nonlinearity, **31**(8), (2018), R189 (53pp).

Common Themes: SLP Problems

- All are singular perturbation problems in 2-D or 3-D domains that require different spatial scales to resolve the localized features.
- SLP theory is a singular perturbation approach that is tailored specifically for resolving small spatial “defects”. Localized regions or “defects” are replaced in the limit $\varepsilon \to 0$ by certain singularity structures defined at “points” for the problem on the macroscale.
- On macroscale, solution is represented by a Green’s function, and Green’s matrices characterize interactions between localized regions.
- For 2-D problems, the expansion parameter is often $\nu = -1/\log \varepsilon$ arising from the $\log r$ behavior of the Green’s function for the Laplacian.
- To achieve high accuracy in 2-D, need a methodology to “sum” the effect of logarithmic interactions $\sum a_j \nu^j$, rather than a finite truncation.

Tutorial Ref: MJW, Asymptotics for Strong Localized Perturbation Theory: Theory and Applications, (lecture notes for 4th winter school in Applied Mathematics, 2010, City U. Hong Kong), (101 pages). (https://personal.math.ubc.ca/ ward/papers/hk_strong.pdf)

End Notes: What does ANY of this have to do with the interests of Julian Cole?

I: Narrow Capture in 3-D

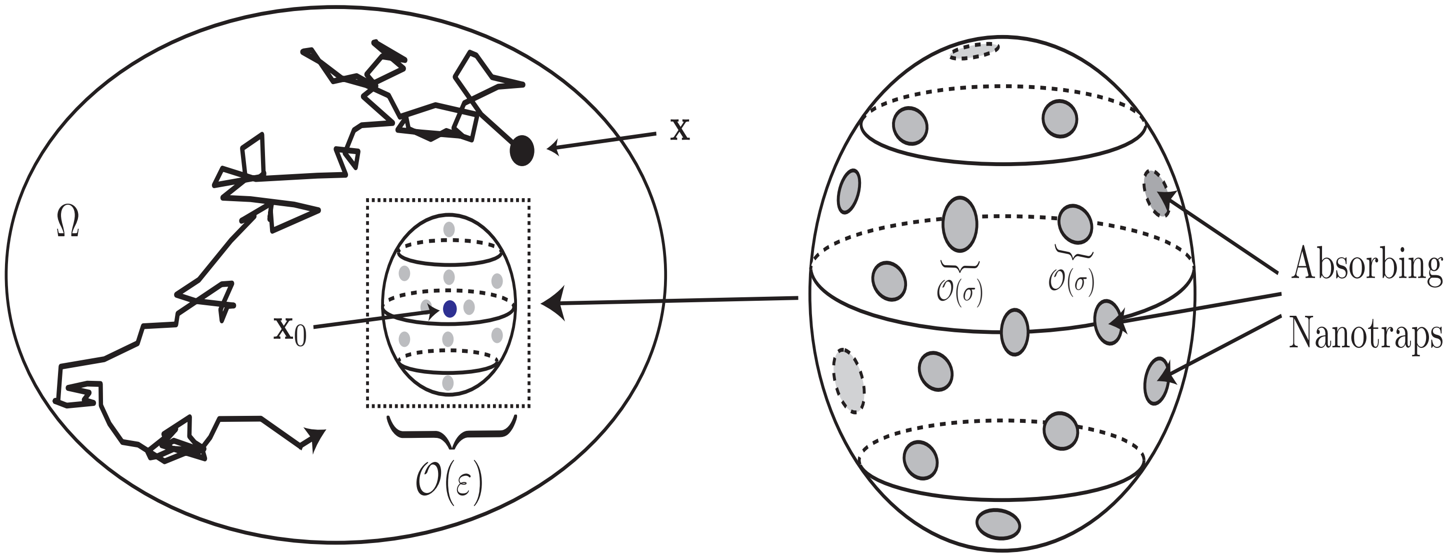

Caption: spherical target Ω_ε of radius $\varepsilon \ll 1$ centered at $\mathbf{x}_0 \in \Omega$, with N locally circular absorbing surface nanotraps(pores) of radii $\sigma \ll \varepsilon$ modeled by a zero Dirichlet condition.

- A particle (protein etc..) undergoes Brownian walk ($dX_t = DdW_t$) until captured by one of the N small absorbing surface nanotraps (applications: antigen binding etc..).
- How long on average does it take to get captured? (MFPT).
- What is the effect on the MFPT of the spatial distribution $\{\mathbf{x}_1, \ldots, \mathbf{x}_N\}$ of the surface nanotraps? Scaling law for $N \to \infty$ but in dilute limit?

The MFPT PDE for Narrow Capture

The Mean First Passage Time (MFPT) T satisfies

$$\Delta T = -\frac{1}{D}\,, \quad \mathbf{x} \in \Omega \backslash \Omega_\varepsilon\,; \quad \partial_n T = 0\,, \quad \mathbf{x} \in \partial\Omega\,,$$
$$T = 0\,, \quad \mathbf{x} \in \partial\Omega_{\varepsilon a}\,; \quad \partial_n T = 0\,, \quad \mathbf{x} \in \partial\Omega_{\varepsilon r}\,,$$

where $\partial\Omega_{\varepsilon a}$ and $\partial\Omega_{\varepsilon r}$ are the absorbing and reflecting part of the surface of the small sphere Ω_ε within the 3-D cell Ω.

- Calculate the averaged MFPT $\bar{T}$ for capture of a Brownian particle.
- $\bar{T}$ depends on the capacitance C_0 of the structured target (related to the Berg-Purcell problem, 1977). This is the “inner” or local problem.
- Derive discrete optimization problems characterizing the optimal $\bar{T}$.

Ref1: [LBW2017] Lindsay, Bernoff, MJW, *First Passage Statistics for the Capture of a Brownian Particle by a Structured Spherical Target with Multiple Surface Traps*, SIAM Multiscale Mod. and Sim. **15**(1), (2017), pp. 74–109.

Ref2: A. Cheviakov, MJW, R. Straube, *An Asymptotic Analysis of the Mean First Passage Time for Narrow Escape Problems: Part II: The Sphere*, Mult. Mod. and Sim. **8**(3), (2010).

Asymptotic Result for the Average MFPT

Using strong localized perturbation theory, for $\varepsilon \to 0$ the average MFPT is

$$\bar{T} \equiv \frac{1}{|\Omega \backslash \Omega_\varepsilon|} \int_{\Omega \backslash \Omega_\varepsilon} T \, d\mathbf{x} = \frac{|\Omega|}{4\pi C_0 D \varepsilon} \left[1 + 4\pi\varepsilon C_0 R(\mathbf{x}_0) + \mathcal{O}(\varepsilon^2) \right],$$

where $R(\mathbf{x}_0)$ is the regular part of the Neumann Green's function for Ω:

$$\Delta G = \frac{1}{|\Omega|} - \delta(\mathbf{x} - \mathbf{x}_0), \quad \mathbf{x} \in \Omega; \quad \partial_n G = 0, \quad \mathbf{x} \in \partial\Omega,$$

$$G(\mathbf{x}; \mathbf{x}_0) \sim \frac{1}{4\pi|\mathbf{x} - \mathbf{x}_0|} + R(\mathbf{x}_0), \quad \text{as} \quad \mathbf{x} \to \mathbf{x}_0; \qquad \int_\Omega G \, d\mathbf{x} = 0.$$

- If Ω is the unit sphere, $R(\mathbf{x}_0)$ can be found analytically in closed form.
- For a cube, $R(\mathbf{x}_0)$ can be found from a rapidly converging infinite series (Ewald summation).
- Otherwise use a boundary-integral solver.

The Inner (Local) Problem Near Target

Let $\Omega_0 \equiv \varepsilon^{-1}\Omega_\varepsilon$, $\mathbf{y} \equiv \varepsilon^{-1}(\mathbf{x}-\mathbf{x}_0)$, and $\Omega_\rho \equiv \{\mathbf{y} \mid |\mathbf{y}| \leq \rho\}$. The capacitance C_0 is defined from an "exterior" problem in potential theory:

$$\Delta w = 0\,, \quad \mathbf{y} \in \mathbb{R}^3 \setminus \Omega_0 \ \text{(outside unit ball)}$$
$$w = 1\,, \quad \mathbf{y} \in \Gamma_a \ \text{(absorbing pores)}$$
$$\partial_n w = 0\,, \quad \mathbf{y} \in \Gamma_r \ \text{(reflecting surface)}$$
$$w \sim \frac{C_0}{|\mathbf{y}|} + \mathcal{O}\left(\frac{1}{|\mathbf{y}|^2}\right)\,, \quad \text{as} \quad |\mathbf{y}| \to \infty\,.$$

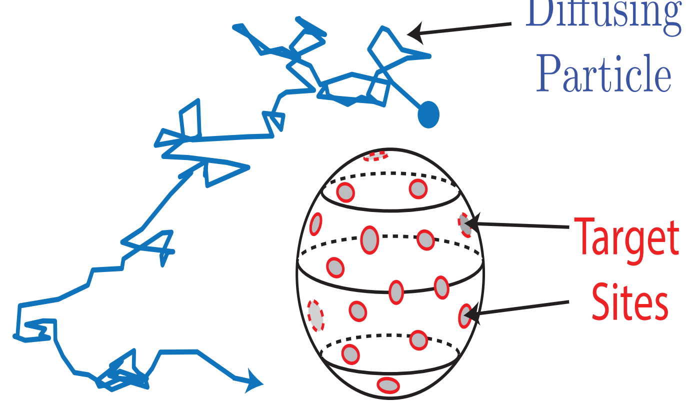

Remarks:

- $C_0 = 1$ if entire surface is absorbing.
- The diffusive flux J into the sphere is

$$J = D\int_{\Gamma_a} \partial_n w\, dS = 4\pi D C_0\,.$$

- The leading-order sub-inner problem near a pore is the electrified disk problem.

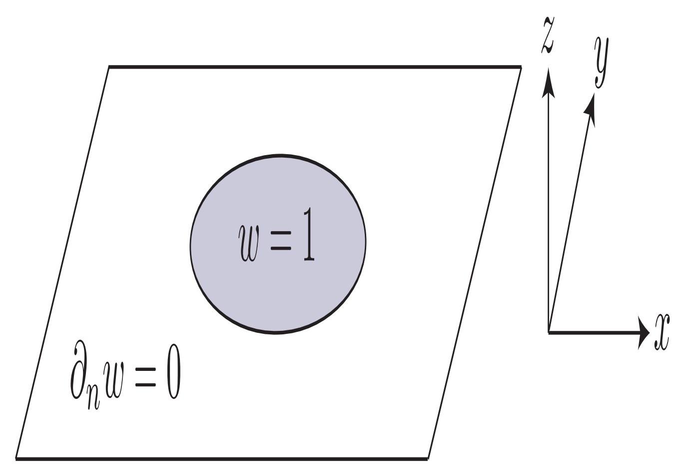

Berg-Purcell Problem: I

This is the Berg-Purcell (BP) problem (*Physics of Chemoreception*, Biophys J. **20**(2), (1977): ≈ 2100 citations)

BP assumed

- $N \gg 1$ disjoint equidistributed small pores.
- common nanopore radius $\sigma \ll 1$.
- dilute fraction limit ($f \equiv N\pi\sigma^2/(4\pi) \ll 1$).

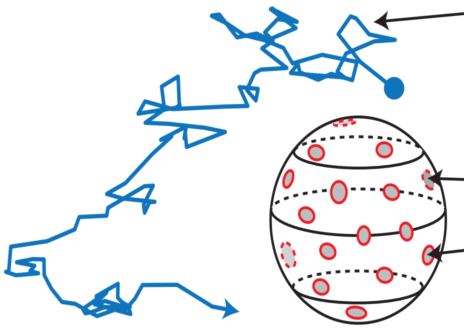

Using a "physically-inspired" derivation, BP postulated that

$$C_{0bp} \approx \frac{N\sigma}{N\sigma + \pi}, \qquad J_{bp} \approx 4\pi D \frac{N\sigma}{N\sigma + \pi} = 4DN\sigma + \mathcal{O}(\sigma^2).$$

Suggests that J is proportional to the total pore perimeter when $\sigma \ll 1$.

Goal: Calculate C_0, and the flux J, for N disjoint pores centered at $\{\mathbf{y}_1, \ldots, \mathbf{y}_N\}$ over the surface. Effect of location and fragmentation? For $N \gg 1$, and "equidistributed" pores derive (and improve) the BP result and get an effective (homogenized) trapping parameter κ for a Robin condition.

Main Result for C_0 and flux J: I

Main Result: For $\sigma \to 0$, [LBW2017] derived that

$$\frac{1}{C_0} = \frac{\pi}{N\sigma}\left[1 + \frac{\sigma}{\pi}\left(\log\left(2e^{-3/2}\sigma\right) + \frac{4}{N}\mathcal{H}(\mathbf{y}_1,\ldots,\mathbf{y}_N)\right) + \mathcal{O}(\sigma^2\log\sigma)\right],$$

$$J = 4DN\sigma\left[1 + \frac{\sigma}{\pi}\log(2\sigma) + \frac{\sigma}{\pi}\left(-\frac{3}{2} + \frac{2}{N}\mathcal{H}(\mathbf{y}_1,\ldots,\mathbf{y}_N)\right) + \cdots\right]^{-1}.$$

The inter-pore interaction energy $\mathcal{H}$, subject to $|\mathbf{y}_j| = 1\ \forall j$, is

$$\mathcal{H}(\mathbf{y}_1,\ldots,\mathbf{y}_N) \equiv \sum_{j=1}^{N}\sum_{k=j+1}^{N} g(|\mathbf{y}_j - \mathbf{y}_k|)\,; \quad g(\mu) \equiv \frac{1}{\mu} + \frac{1}{2}\log\mu - \frac{1}{2}\log(2+\mu)\,.$$

Here $\mathbf{y}_j$ for $j = 1,\ldots,N$ are the nanopore centers with $|\mathbf{y}_j| = 1$.

Remarks:

- Flux J minimized when $\mathcal{H}$ minimized
- $g(\mu)$ is monotone decreasing, positive, and convex.
- Indicates that optimal configuration should be (roughly) equidistributed.

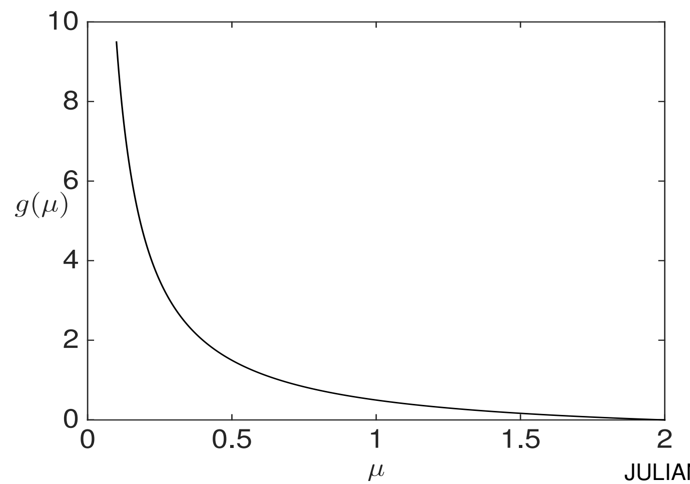

Main Result for C_0 and flux J: II

Note: $g(|\mathbf{y}_j - \mathbf{y}_k| = 2\pi G_s(\mathbf{y}_j;\mathbf{y}_k)$, G_s is the surface-Neumann G-function

$$G_s(\mathbf{y}_j;\mathbf{y}_k) = \frac{1}{2\pi}\left[\frac{1}{|\mathbf{y}_j - \mathbf{y}_k|} - \frac{1}{2}\log\left(\frac{1 - \mathbf{y}_j\cdot\mathbf{y}_k + |\mathbf{y}_j - \mathbf{y}_k|}{|\mathbf{y}_j| - \mathbf{y}_j\cdot\mathbf{y}_k}\right)\right].$$

Key steps in SLP analysis for C_0:

- Asymptotic expansion of global (outer) solution and local (inner) solutions near each pore (using tangential-normal coordinates).
- The surface G_s-function has a subdominant logarithmic singularity on the boundary (related to surface diffusion). This fact requires adding "logarithmic switchback terms in σ" in the outer expansion.
- The leading-order local solution is the tangent plane approximation and yields electrified disk problem in a half-space, with (local) capacitance $c_j = 2\sigma/\pi$.
- **Key:** Need corrections to the tangent plane approximation in the inner region near the pore. This higher order term in the inner expansion satisfies a Poisson-type problem, with monopole far-field behavior.
- Asymptotic matching and solvability conditions yield $1/C_0$.

Discrete Energy: Equidistributed Points

Find global minimum $\mathcal{H}_{\min}$ of $\mathcal{H}$ when $N \gg 1$

$$\mathcal{H} = \sum_{j} \sum_{k \neq j} g(|\mathbf{y}_j - \mathbf{y}_k|) \,, \quad \text{where} \quad g(\mu) \equiv \frac{1}{\mu} + \frac{1}{2} \log \left(\frac{\mu}{2+\mu} \right) .$$

- What is asymptotics of $\mathcal{H}_{min}$ as $N \to \infty$?
- For large N, many local minima, so finding global min is difficult.
- Cannot tile a spherical surface with hexagons (must have defects).
- A new cousin of the classic Fekete point problems of minimizing pure Coulombic energies on the sphere (Smale's 7th problem).

Three Coverings of $N = 800$ points

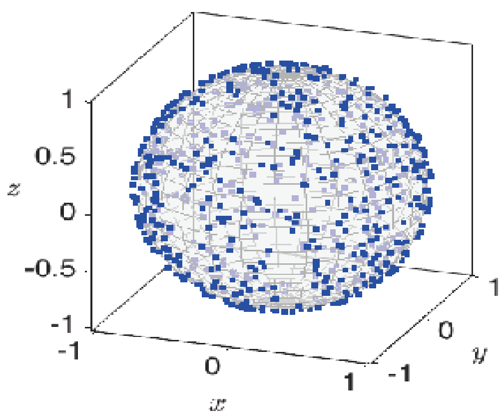

Uniform Random
Not Great

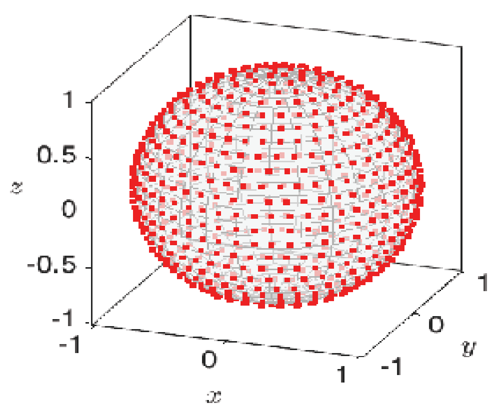

Equispaced in (θ, ϕ)
Better

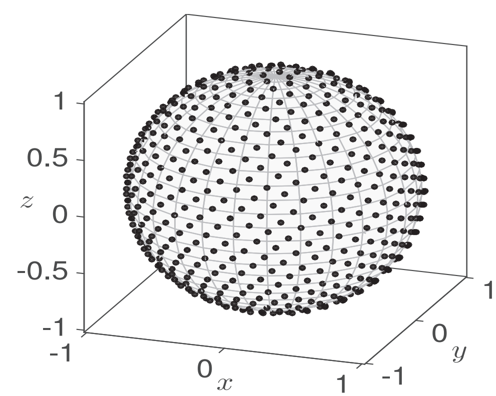

Fibonacci Spirals
Best (so far...)

Scaling Law: Equidistributed Points

Formal Large N Limit: For N large and "equidistributed points", we have

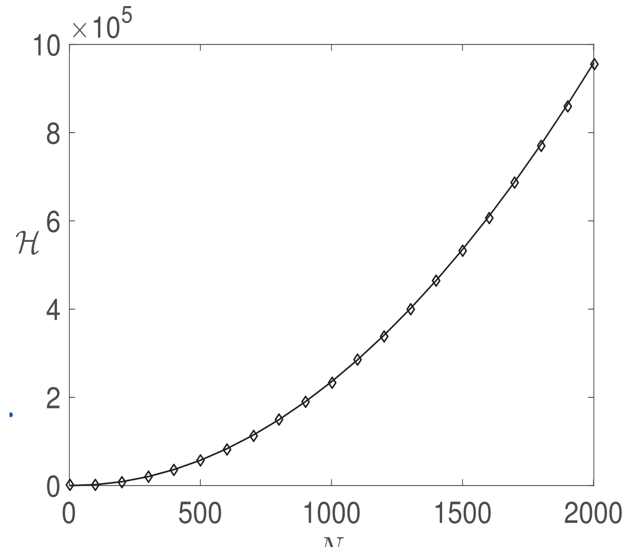

$$\mathcal{H}_{min} \sim \frac{N^2}{4} - d_1 N^{3/2} + \frac{N}{8}\log N + d_2 N + d_3 N^{1/2} + \cdots,$$

with $d_1 = .5$, $d_2 = .125$ and $d_3 = .25$.

Main Result (Scaling Law): For $N \gg 1$, but small pore surface area fraction $f = \mathcal{O}(\sigma^2 \log \sigma)$ and with equidistributed pores, the optimal C_0 and J are

$$\frac{1}{C_0} \sim 1 + \frac{\pi\sigma}{4f}\left(1 - \frac{8d_1}{\pi}\sqrt{f} + \frac{\sigma}{\pi}\log\left(\beta\sqrt{f}\right) + \frac{2d_3\sigma^2}{\pi\sqrt{f}}\right), \quad \beta \equiv 4e^{-3/2}e^{4d_2},$$

$$J \sim 4\pi D\left[1 + \frac{\pi\sigma}{4f}\left(1 - \frac{8d_1\sqrt{f}}{\pi} + \frac{\sigma}{\pi}\log\left(\beta\sqrt{f}\right) + \frac{2d_3\sigma^2}{\pi\sqrt{f}}\right)\right]^{-1}.$$

- Berg-Purcell result is the leading-order term.
- Our analysis yields correction terms for the sphere. Most notable is the $\sqrt{f}$ term, where $f \equiv N\sigma^2/4$.

Compare Scaling Law with Full Numerics

Compare full numerics (Bernoff-Lindsay) with the asymptotic scaling law

$$J \sim 4\pi D \left[1 + \frac{\pi\sigma}{4f} \left(1 - \frac{8d_1\sqrt{f}}{\pi} + \frac{\sigma}{\pi} \log\left(\beta\sqrt{f}\right) + \frac{2d_3\sigma^2}{\pi\sqrt{f}} \right) \right]^{-1} .$$

Fix 2% pore coverage ($f = 0.02$) and choose spiral Fibonacci points.

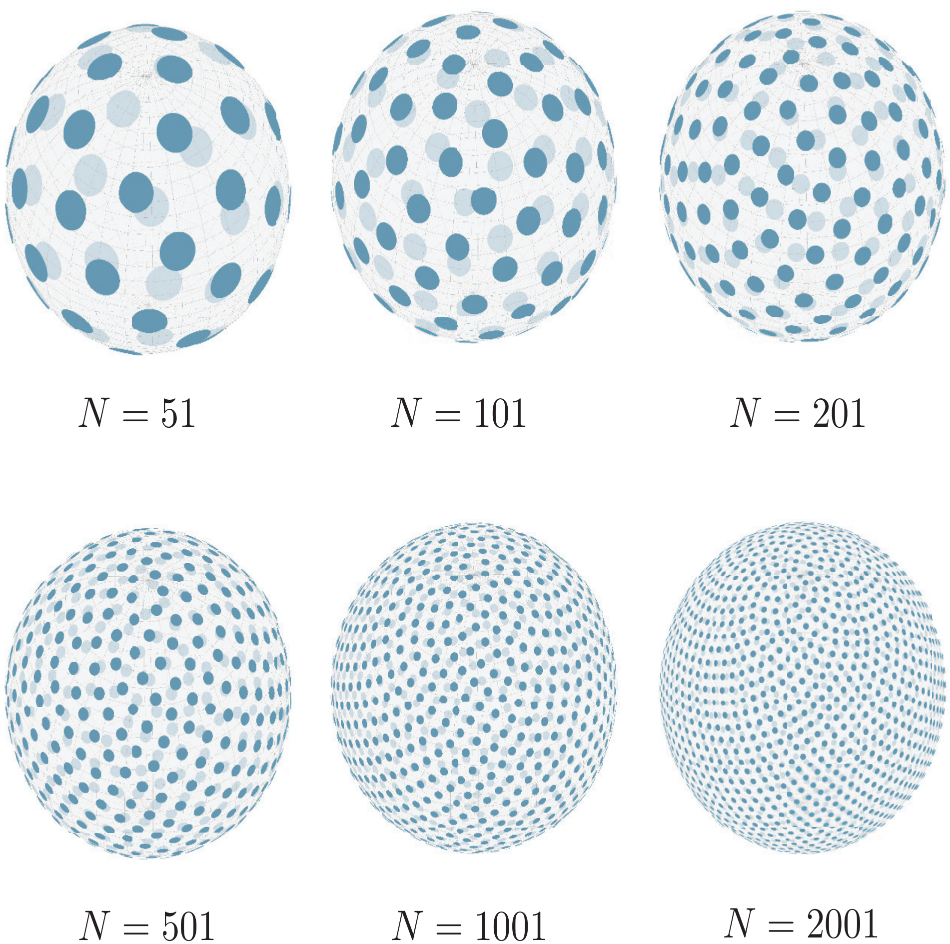

N	$\mathcal{E}_{\text{rel}}$
51	1.02%
101	0.90%
201	0.76%
501	0.58%
1001	0.37%
2001	0.34%

Caption: $f = 0.02$ (2% pore coverage). Scaling law accurately predicts the flux to the target for the biological parameter range $f = 0.02$ and $N = 2001$.

Effective Robin Condition: Leakage κ_h

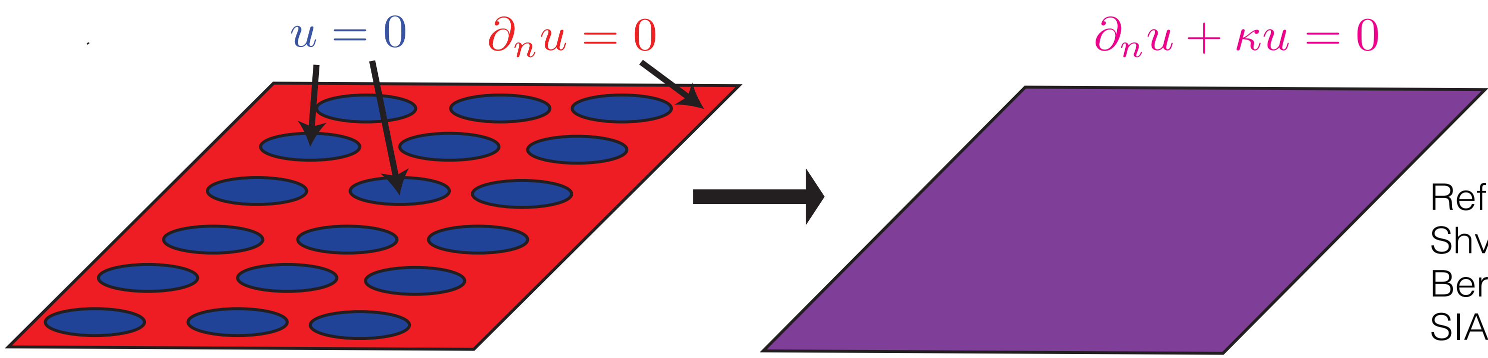

Ref: Muratov, Shvartsmam, Berezhkovskii, SIAM MMS 2006.

Consider the planar case with σ pore radius and f coverage. Previous empirical laws (Berezhkovskii 2013) for a hexagonal arrangement

$$\kappa = \frac{4Df}{\pi\sigma}\chi(f)\,, \qquad \chi(f) = \frac{1 + 1.37\sqrt{f} - 2.59 f^2}{(1-f)^2}\,.$$

Our homogenized Robin condition: use scaling law for C_0 and find κ_h from

$$\Delta v_h = 0\,, \quad |\mathbf{y}| > 1\,; \quad \partial_n v_h + \kappa_h v_h = 0\,, \quad |\mathbf{y}| = 1\,; \quad v_h(\mathbf{y}) \sim \frac{1}{|\mathbf{y}|} - \frac{1}{C_0}\,, \quad |\mathbf{y}| \to \infty\,.$$

For the unit sphere, and in terms of d_1, d_2, d_3 and $\beta \equiv 4e^{-3/2}e^{4d_2}$, we get

$$\kappa_h \sim \frac{4Df}{\pi\sigma}\left[1 - \frac{8d_1}{\pi}\sqrt{f} + \frac{\sigma}{\pi}\log\left(\beta\sqrt{f}\right) + \frac{2d_3\sigma^2}{\pi\sqrt{f}}\right]^{-1} \approx \frac{4Df}{\pi\sigma}\left[1 + 1.41\sqrt{f} + \cdots\right]\,.$$

Remarks and Further Directions

- **Approximation theory:** SLP theory has led to a new discrete variational problem related to the classic Fekete point problem: Challenge: derive rigorous large N scaling law.
- **Numerics for Full PDE (Sphere):** Boundary integral methods challenging owing to $N \gg 1$ and edge singularities at Dirichlet/Neumann corners (*Lindsay, Bernoff [LBW2017] and L. Greengard, J. Kaye JCP X 5 10047 (2020) (fast potential theory)*).

Further Directions:

- What about full time-dependent probability density? (Some recent results in 2-D *Cherry, Lindsay, Hernandez, and Quaife*, archive)
- The effect of more realistic trap models? (i.e. finite receptor kinetics (**Ref:** *Handy, Lawley*, Biophys. J. **120**(11), 2021))
- Capacitance of a non-spherical surface containing N nanopores: **Asymptotics:** Local analysis near a pore is possible, but no explicit globally-defined surface Neumann Green's function. Need detailed behavior of the local singularity (microlocal analysis techniques? (*M. Nursultanov, L. Tzou, and J. Tzou, J. Math. Pures. Appl. (2021)*))

III: Localized Spots for Singularly Perturbed RD Models

$$v_t = \varepsilon^2 \triangle v + g(u,v)\,; \quad \tau u_t = D \triangle u + f(u,v)\,, \qquad \mathbf{x} \in \Omega \in \mathbb{R}^2\,.$$

Assume $\varepsilon \ll 1$ and $D = \mathcal{O}(1)$. **Key:** Since $\varepsilon \ll 1$, v can be localized in space as a spot pattern, i.e. concentration at a discrete set of points.

Prototypical Kinetics: Brusselator, Gray-Scott, GM, Schnakenberg, etc..

Specific Applications: Biological morphogenesis, Self-replicating patterns in chemical interactions, plant root-hair formation driven by auxin gradient, hot-spot patterns of urban crime, vegetation patches in semi-arid environments (spatial ecology).

Two Distinct Methodologies

- **Classical Approach**: stability of spatially uniform states, Turing and weakly nonlinear analysis of small amplitude patterns, leading to normal form amplitude equations. Not so useful in singular limit.
- **Localized Patterns:** "Far-from equilibrium patterns" (Y. Nishiura) consisting of "particles" (v) interacting through a "diffusion field" (u).
  - **Key:** SLPT: $\nu = -1/\log \varepsilon$ is expansion parameter.
  - Spot interactions via Green's functions and Green's matrices
  - Optimization of stability thresholds yield new (discrete) VPs.

Spotty Vegetation Patterns in 2-D

The dimensionless extended Klausmeir-model in 2-D (with no flux BC):

$$v_t = \epsilon^2 \Delta v - mv + uv^2 \,, \quad u_t = \Delta u + H u_x - u + a - \varepsilon^{-2} uv^2 \,, \quad \text{in} \quad \Omega = [0,1]^2 \,.$$

- v (biomass) and u (surface water).
- m mortality rate of vegetation, a is rainfall rate (in regime where striped patterns do not exist).
- $H > 0$ uniform terrain slope in x direction.
- $\epsilon \ll 1$ since water diffuses much faster than biomass.
- v concentrates on points as $\epsilon \to 0$ (i.e. spot pattern).

Framework: Develop a mathematical theory to analyze the existence, stability, and dynamics, of localized “far-from equilibrium” spot patterns.

- **Q1:** Localized patterns can undergo instabilities (competition, self-replication, etc.) 2-D NLEP theory: Wei-Winter-MJW
- **Q2:** If no instabilities, derive a DAE system for the slow time evolution of the center of the spots. (SLPT key here).

T. Wong, MJW *Dynamics of Patchy Vegetation Patterns in the Two-Dimensional Generalized Klausmeier Model*, to appear, DCDS Series S, (2022), (47 pages).

A Decreasing Rainfall Rate and Spot Annihilation

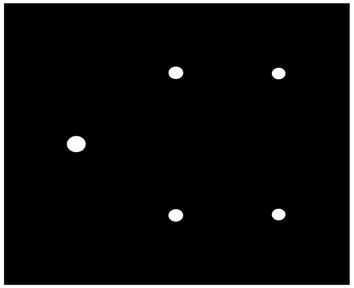
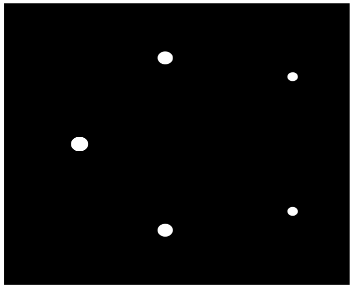
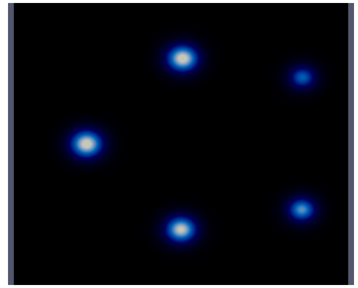

(a) $t = 5$ **(b)** $t = 400$ **(c)** $t = 1000$

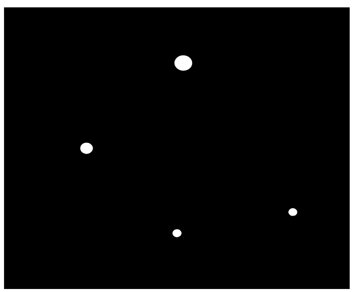
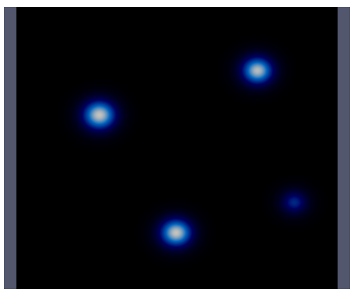
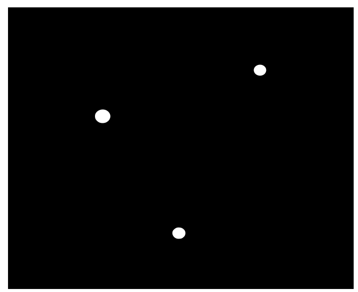

(d) $t = 1010$ **(e)** $t = 1275$ **(f)** $t = 1285$

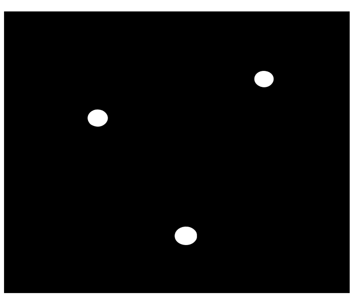
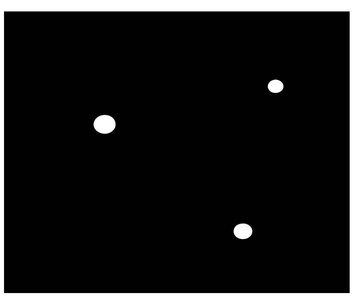
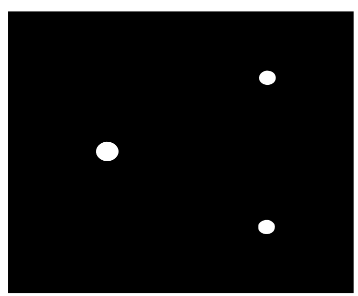

(g) $t = 1300$ **(h)** $t = 1585$ **(i)** $t = 3390$

Left: Snapshots of PDE results with $\varepsilon = 0.02$, $H = 1.0$, and a dynamic rainfall rate $a = \max(70 - 0.01t, 55)$. Vegetation patches are slowly annihilated.

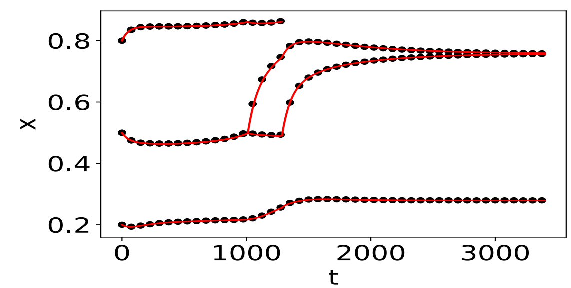

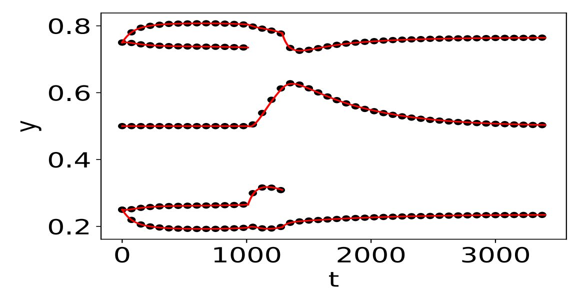

Above: Spot trajectories from the DAE (arising from SLPT) and the PDE compare very well before and after spot-annihilation events.

III: Diffusion-Mediated Communication

Formulate and analyze a 2-D PDE-ODE model of m dynamically active small stationary "cells", with arbitrary intracellular kinetics (ODE), that are coupled spatially by a linear bulk-diffusion field (PDE) "autoinducer" (AI).

Quorum sensing (QS): collective behavior triggered as m exceeds a threshold. (Usually studied in the well-mixed limit)

Diffusion-Mediated Communication: collective behavior resulting from spatial effects from diffusive transport. (Spatial clustering of cells, shielding effects, spatially isolated cells, signalling gradient).

- **Oscillatory:** sudden emergence of intracellular oscillations as m increases (eg: glycolysis, social amoeba, catalyst bead particles).
  - With no bulk coupling, "cells" are quiet. Oscillations and ultimate sychronization occurs via a switchlike Hopf bifuraction response.
- **Transitions:** between small and large amplitude bistable steady-states as m increases (eg: bioluminescence, *Pseudomonas aeruginosa*).
  - As m increases, or cells become spatially clustered, there can be a passage past a saddle-node point leading to a bistable transition.

Modeling Frameworks? Kuramoto? (ODE only); RD system? (phemenological); Homogenization? (possible); Agent-Based-Lattice-Simulations? (please no!).

Formulation of the PDE-ODE Model I

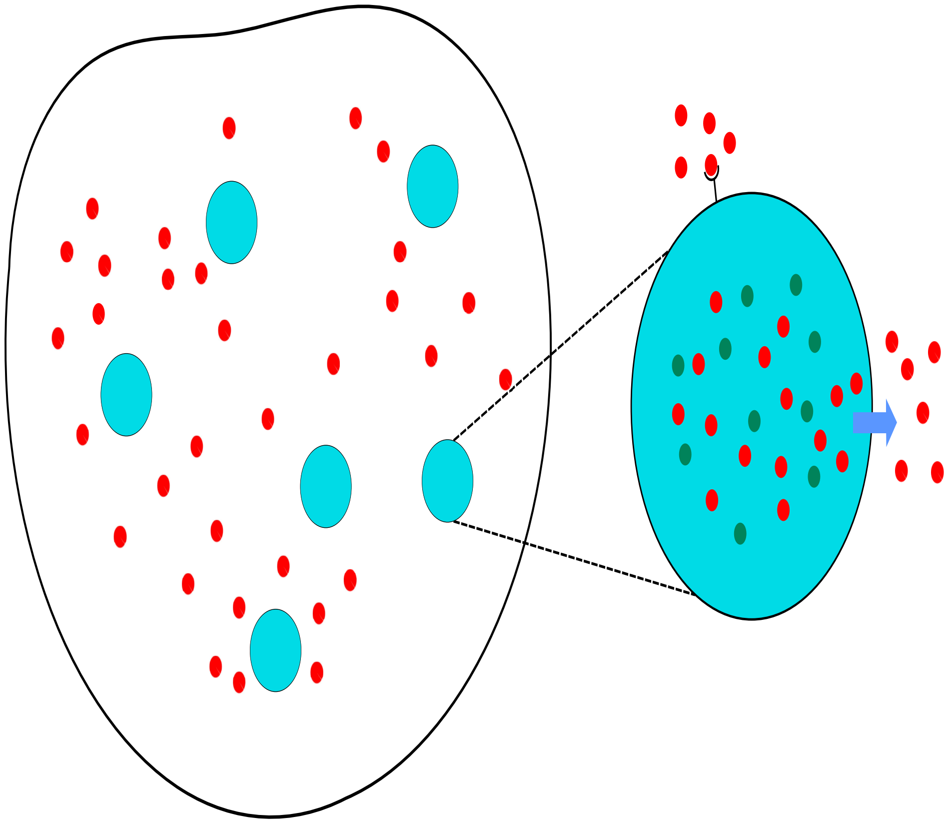

- The m cells are circular and each contains n chemicals $\mu_j = (\mu_{1j}, \ldots, \mu_{nj})^T$. When isolated from the bulk they interact via ODE's $\mathbf{d}\mu_j/dt = k_R \mathbf{F}_j(\mu_\mathbf{j})$.
- A scalar bulk diffusion field (autoinducer) diffuses in the space between the cells via

$$\mathcal{U}_T = D_B \Delta_{\mathbf{X}} \mathcal{U} - k_B \mathcal{U} \, .$$

- There is an exchange across the cell membrane, regulated by permeability parameters, between the autoinducer and one intracellular species (Robin condition).

Scaling Limit: $\epsilon \equiv \sigma/L \ll 1$, where L is lengthscale for Ω.

Parameters: Bulk diffusivity D_B, bulk decay rate k_B, intracellular reaction rate k_R.

Framework inspired by: **Refs:** J. Muller, C. Kuttler, et al. JMB **53** (2006); J. Muller, H. Uecker, JMB **67** (2013).

Formulation of the PDE-ODE Model II

Dimensionless Formulation: The concentration of signalling molecule $U(\boldsymbol{x}, t)$ in the bulk satisfies the PDE:

$$\tau U_t = D\Delta U - U \,, \qquad \boldsymbol{x} \in \Omega \backslash \cup_{j=1}^{m} \Omega_{\epsilon_j} \,; \quad \partial_n U = 0 \,, \quad \boldsymbol{x} \in \partial\Omega \,,$$

$$\epsilon D \partial_{n_j} U = d_{1j} U - d_{2j} u_j^1 \,, \qquad \boldsymbol{x} \in \partial\Omega_{\epsilon_j} \,, \quad j = 1, \ldots, m \,.$$

The cells are disks of radius $\epsilon \ll 1$ so that $\Omega_{\epsilon_j} \equiv \{\boldsymbol{x} \,|\, |\boldsymbol{x} - \boldsymbol{x}_j| \leq \epsilon\}$.

Inside each cell there are n interacting species $\boldsymbol{u}_j = (u_j^1, \ldots, u_j^n)^T$, with intracellular dynamics for each $j = 1, \ldots, m$,

$$\frac{d\boldsymbol{u}_j}{dt} = \boldsymbol{F}_j(\boldsymbol{u}_j) + \frac{\boldsymbol{e}_1}{\epsilon\tau} \int_{\partial\Omega_{\epsilon_j}} (d_{1j} U - d_{2j} u_j^1) \, ds \,, \qquad \boldsymbol{e}_1 \equiv (1, 0, \ldots, 0)^T \,.$$

Remark: The time-scale is measured wrt intracellular kinetics. The dimensionless bifurcation parameters are: d_{1j}, d_{2j} (permeabilities); τ (reaction-time ratio); D (effective diffusivity);

$$\tau \equiv \frac{k_R}{k_B} \,, \qquad D \equiv \left(\frac{\sqrt{D_B/k_B}}{L} \right)^2 \,.$$

Role of Intracellular Kinetics F_j

- **Triggered Oscillations:** Intracellular kinetics are a conditional oscillator: Quiescent when uncoupled from the bulk. Bulk coupling triggers a Hopf bifurcation for the collection of cells. (Sel'kov kinetics $n = 2$)
  Refs: J. Gou, MJW, JNLS, **26**(4), (2016); S. Iyaniwura, MJW, SIADS, **20**(1), (2021).

- **Transitions:** Intracellular kinetics have a saddle-node structure and bistable states when uncoupled from bulk. Bulk-coupling induces an effective bifurcation parameter, depending on m, that can sweep past fold points (Lux kinetics $n = 4$) **Refs:** W. Ridgway, B. Wetton, MJW, JMB, (2022).

Two key regimes for effective bulk diffusivity D:

- $D = \mathcal{O}(1)$; Effect of spatial distribution of cells is a key factor whether either intracellular oscillations or saddle-node transitions occur.

- $D = \mathcal{O}(\nu^{-1})$ with $\nu = -1/\log \epsilon$; PDE-ODE system can be reduced to a limiting ODE system where there is a weak effect of cell locations.
  - $D \to \infty$; The classic “well-mixed” regime: Obtain an ODE system with global coupling and no spatial effects. (QS behavior).

Analysis: Use SLPT to construct steady-states and to analyze the linear stability problem. Derive the reduced ODE system for $D = \mathcal{O}(\nu^{-1})$. Ensure that the asymptotic theory effectively sums all $\nu = -1/\log \epsilon$ terms.

Sel'kov Kinetics: $m = 10$ cells with two clusters

Q: what is the effect of varying the influx permeability rate d_1 into the cells from the bulk medium when $D = D_0/\nu$? Here Ω is unit disk and $\varepsilon = 0.05$.

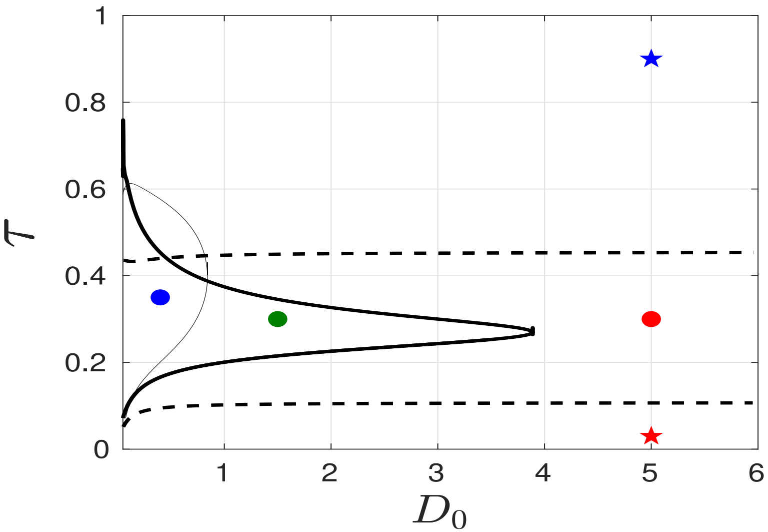

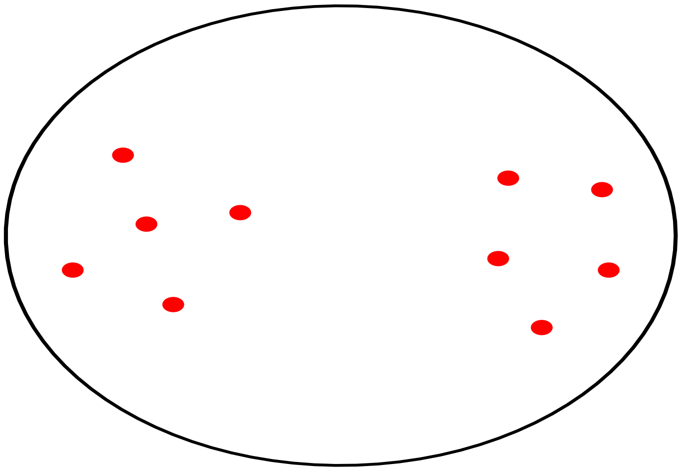

Caption: HB boundaries in the τ versus D_0 plane for $m = 10$ cells with two groups/clusters of cells. Dashed curve: identical cells with $d_1 = 0.8$. Thin solid: $d_1 = 0.8$ for the first group and $d_1 = 0.4$ for second group. Heavy solid: non-identical cells with d_1 uniformly in $0.4 \leq d_1 \leq 0.8$. FlexPDE simulations given below at indicated points.

Key: Oscillations predicted within the lobes. HB boundaries depend sensitively on d_1. Computed from the roots of nonlinear matrix problem $\det(\mathcal{M}(\lambda; \tau, D)) = 0$ with $\lambda = i\lambda_I$ that arises from SLPT reduction

Two Identical Clusters: Red Dot

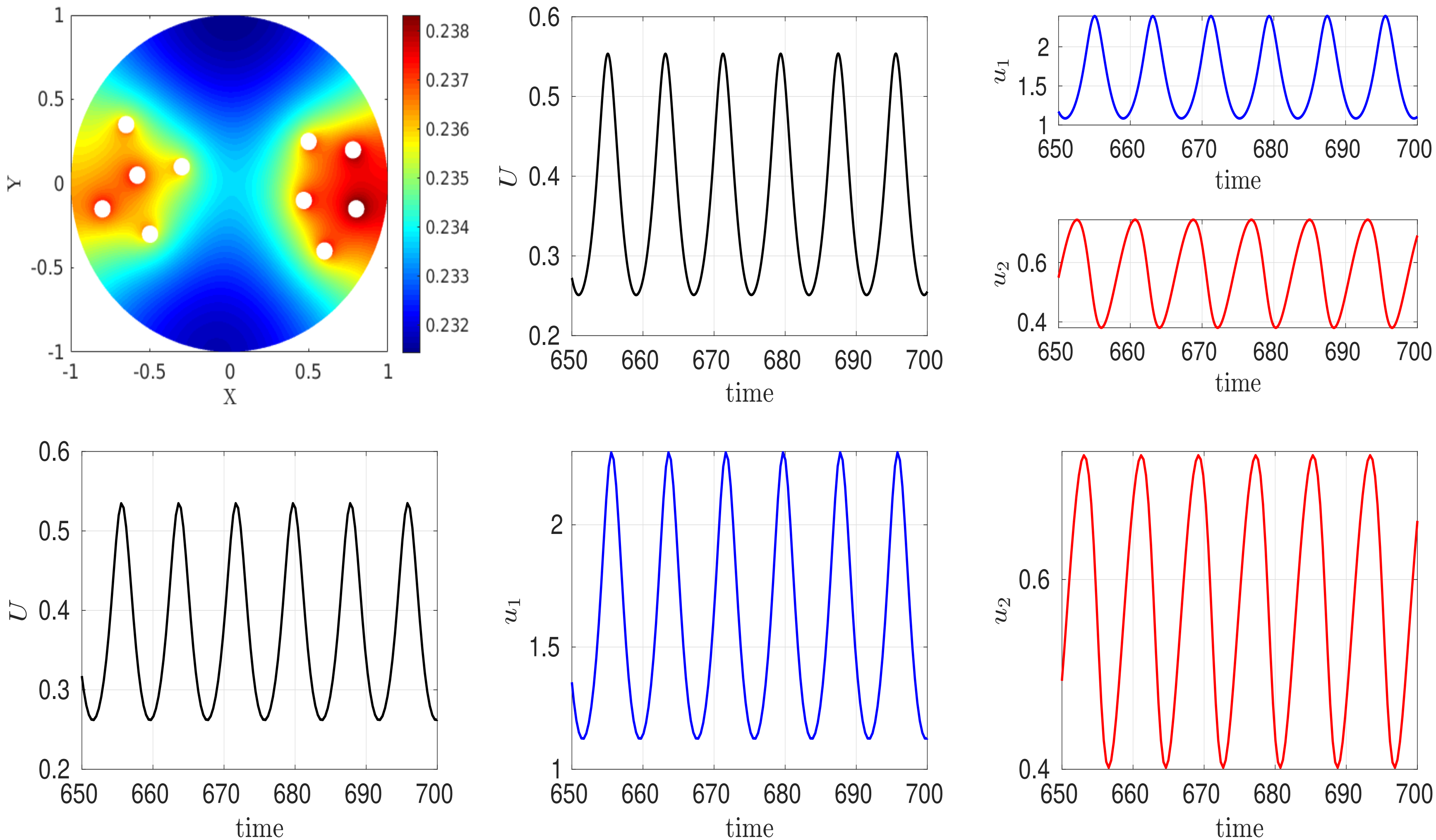

Caption: Top row: FlexPDE results at $(D_0, \tau) = (5.0, 0.3)$ with identical influx rates $d_{1j} = 0.8$ for $j = 1, \ldots, m$. Lower row: $\bar{U}$, u_1, and u_2, as computed from the ODEs.

Observe: Nearly synchronized intracellular oscillations.

Two Distinct Clusters: Blue Dot

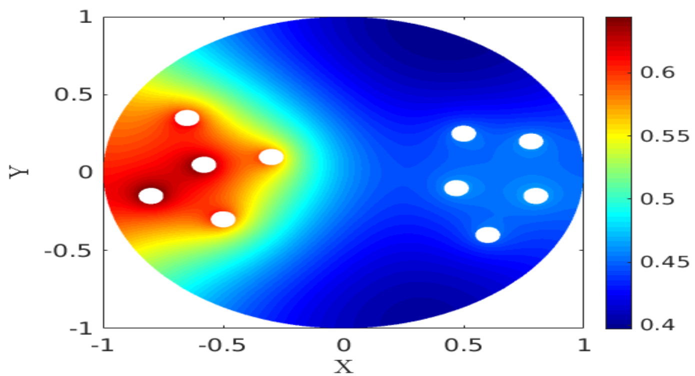

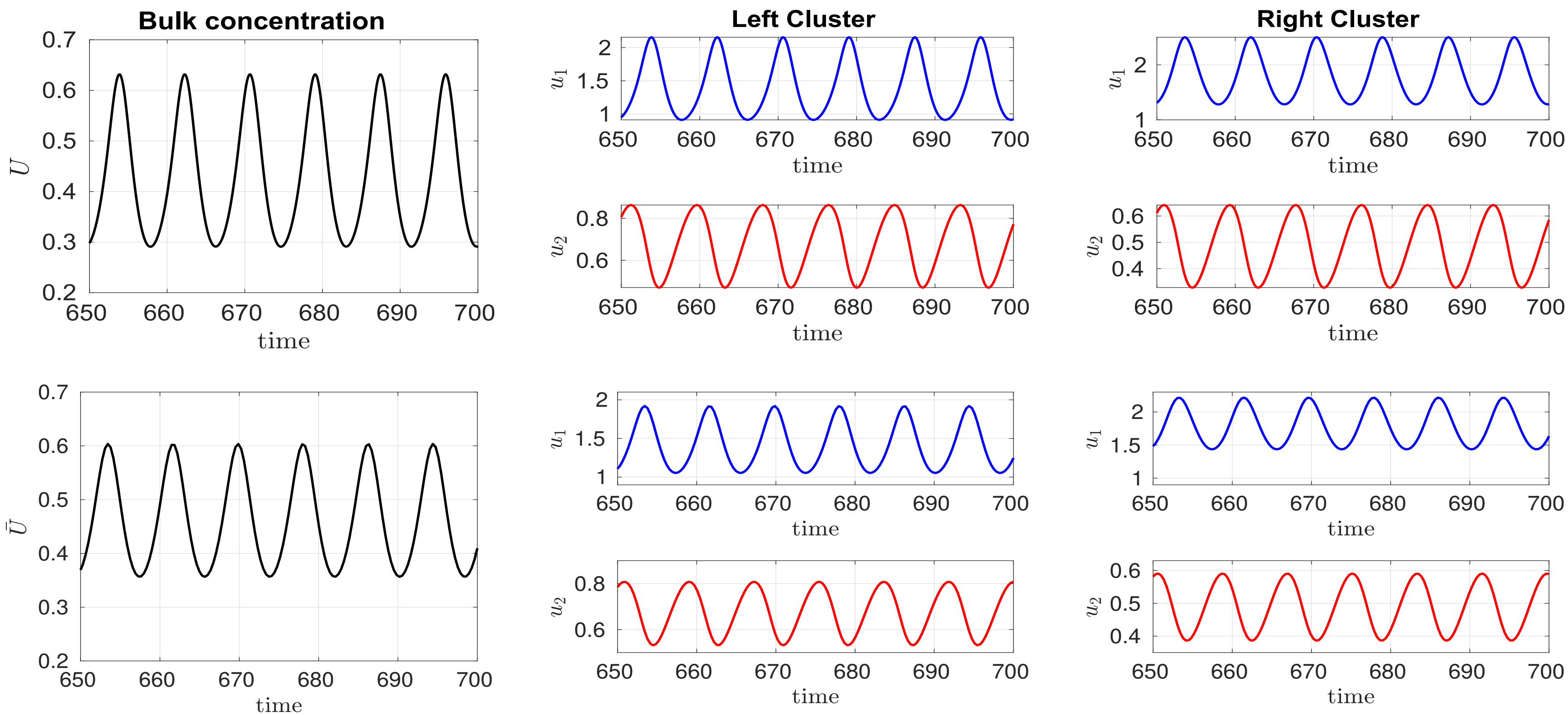

Caption: Top/ middle rows: FlexPDE results at $(D_0, \tau) = (0.4, 0.35)$. Cells in the left and right clusters have $d_1 = 0.4$ and $d_1 = 0.8$, resp. Lower row: $\bar{U}$, u_1, and u_2, from the ODEs.

Two Identical Clusters: Red/Blue Stars

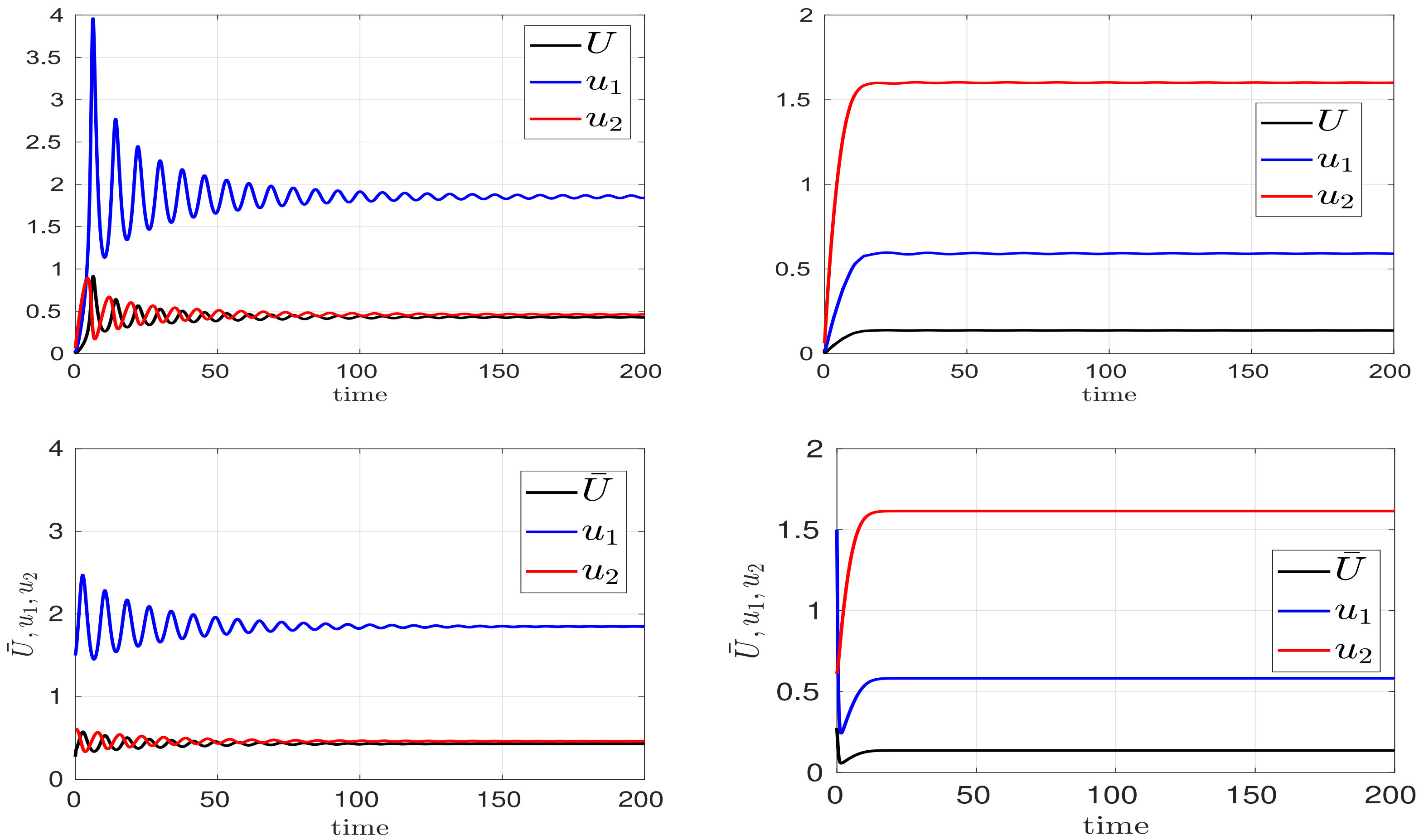

Caption: Top Row: FlexPDE results at the blue star with $(D_0, \tau) = (5.0, 0.9)$ (left panel) and at the red star with $(D_0, \tau) = (5.0, 0.03)$ (right panel). Identical influx rates $d_1 = 0.8$ for all cells. Lower row: $\bar{U}$, u_1, and u_2, from the ODE system.

Observe: oscillatory versus monotonic approach to the steady-state.

End Notes: Julian Cole

Julian made seminal contributions across MANY specific areas (transonic flow and aerodynamics, perturbation theory, symmetry analysis, fluids).

70th B-day collection: ***"Mathematics is for Solving Problems"***, **eds. V. Roytburd, P. Cook, M. Tulin.** (SIAM Press).

The Low Re Quagmire: In the late 1950's and early 1960s, there was an intense focus at Caltech (GALCIT) and Cambridge on using singular perturbation methods for accurately calculating the drag coefficient C_D for a long cylinder of circular cross-section in a steady-state low Re flow with free stream (Kaplun, Lagerstrom, Proudman-Pearson, Van Dyke, Cole).

- For $\varepsilon \equiv \text{Re} \to 0$, they obtained $C_D \sim 4\pi\varepsilon^{-1}F(\varepsilon)$, where $F(\varepsilon)$ is an infinite logarithimic series in powers of $-1/\log\varepsilon$.
- Only three coefficients can be calculated analytically and this severe truncation for C_D agrees rather poorly with the experimental results.
- Challenge: infinite log expansion converges for ε small or is it only an asymptotic series (optimal number of terms)? If it converges, can we sum it? What about transcendetally small effects?
- As a Szego PDF with my mentor Joe Keller from 1988-1991, M. Van Dyke (Aero, Stanford) would routinely still lament this challenge to us.

SLPT and the Low Re Drag Problem I

For steady-state low Re flow over a circular cylinder with a Navier (rough boundary) condition, the 2-D streamfunction ψ satisfies

$$\Delta_r^2 \psi = -\varepsilon\, J_r\left[\psi, \Delta_r \psi\right]\,, \quad r > 1\,; \qquad \psi \sim r \sin\theta\,, \ \text{ as } \ r \to \infty\,,$$

$$\psi = 0\,, \quad l\psi_{rr} - \left(\frac{l}{r} + 1\right)\psi_r = 0\,, \ \text{ on } \ r = 1\,.$$

Here $\varepsilon \equiv U_\infty L \rho_f / \mu \ll 1$ is the Reynolds number, $l = l_c/L$ is the dimensionless Navier sliplength and $J_r\left[a, b\right] \equiv r^{-1}\left(\partial_r a\, \partial_\theta b - \partial_\theta a\, \partial_r b\right)$.

SLPT Approach: Let $\rho = \varepsilon r$, and let $\Psi_H \equiv \Psi_H(\rho, \theta; S)$ satisfy

$$\Delta_\rho^2 \Psi_H = -J_\rho\left[\Psi_H, \Delta_\rho \Psi_H\right]\,, \quad \rho > 0\,; \qquad \Psi_H \sim \rho \sin\theta\,, \ \text{ as } \ \rho \to \infty\,,$$

$$\Psi_H \sim \left[S \log\rho + R(S) + o(1)\right] \rho \sin\theta\,, \ \text{ as } \ \rho \to 0\,; \quad (\text{"}sing.structure\text{"}).$$

For a range of S values, we must compute the regular part $R = R(S)$.

Stokes (inner) region: Let $r = \mathcal{O}(1)$, we set $\psi = S\psi_c$, where

$$\Delta_r^2 \psi_c = 0\,, \quad r > 1\,; \qquad \psi_c \sim r \log r \sin\theta\,, \ \text{ as } \ \rho \to \infty\,,$$

$$\psi_c = 0\,, \quad l\psi_{crr} - \left(\frac{l}{r} + 1\right)\psi_{cr} = 0\,, \ \text{ on } \ r = 1\,.$$

SLPT and the Low Re Drag Problem II

which has the solution

$$\psi_c = \left[r \log r + c(r - r^{-1}) \right] \sin\theta \,, \quad \text{where} \quad c \equiv -\frac{1}{2+4l} \,.$$

By asymptotic matching the regular parts: To all orders in ν, C_D satisfies

$$C_D \sim 4\pi\varepsilon^{-1} \nu R\left[S(\nu)\right] \,, \quad \text{where} \quad \frac{S}{R(S)} = \nu \equiv -\frac{1}{\log\left[\varepsilon e^{-c}\right]} \ll 1 \,.$$

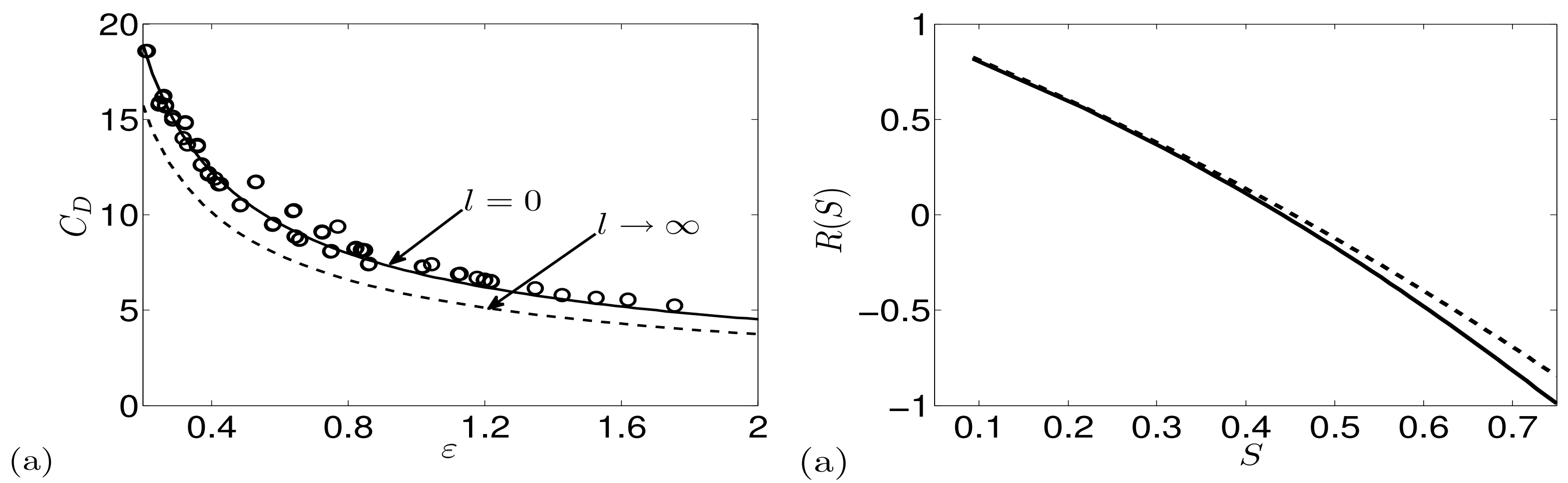

Left: C_D vs. ε (solid and dashed) with experimentals (Tritton). Right: $R(S)$ computation.

Refs: Kropinski, MJW, J. Keller, SIAP **55**(6), (1995); S. Hormozi, MJW, J. Eng. Math., **102**(2), (2017). **Open PDE challenge:** Prove that $R(S)$ is analytic for S small.

Final Comments

- Although **singular perturbation theory** is a **classic but OLD** topic in Applied Math, it still provides a highly relevant methodology for revealing solution behavior for ODEs and PDEs arising in modern applications.
- Indeed the spirit of **"Mathematics is for Solving Problems"** (Julian Cole) is alive and well in SLP theory illustrated by the applications it has been applied to. However, incorporating results and techniques from the "purer" side (PDE theory, approximation theory, spectral theory, microlocal analysis), as well as contemporary numerical methodologies, is often very relevant and powerful.
  - For the QS problem a key computational challenge is finding λ such that $\det \mathcal{M}(\lambda) = 0$ for possibly large non-Hermitian matrices with no simple dependence on λ (Betze, Highan, Mehrmann)
- **If anyone out in zoomland has a specific problem for which SLPT might be useful you know where to find me.**

Thanks to SIAM for the honour of the Julian Cole Lectureship!